



In situ pressure-induced solid-state amorphization in $\text{Sm}_2(\text{MoO}_4)_3$, $\text{Eu}_2(\text{MoO}_4)_3$ and $\text{Gd}_2(\text{MoO}_4)_3$ crystals: chemical decomposition scenario

Vladimir Dmitriev^{a,b,*}, Vitaly Sinitsyn^c, Ruben Dilanian^c, Denis Machon^b,
Alexey Kuznetsov^a, Eugeny Ponyatovsky^c, Guy Lucazeau^b, Hans Peter Weber^{a,d}

^aGroup “Structure of Materials under Extreme Conditions”, Swiss–Norwegian Beam Lines at ESRF, BP 220, F-38043 Grenoble, France

^bLEPMI/ENSEEG, F-38402 Saint Martin d’Heres, France

^cInstitute of Solid State Physics of the Russian Academy of Sciences, Chernogolovka, Moscow District 142432, Russian Federation

^dInstitute of Crystallography, University of Lausanne, CH-1015 Lausanne, Switzerland

Received 15 April 2002; accepted 7 May 2002

Abstract

The effect of pressure on the phase transformations in $\text{Sm}_2(\text{MoO}_4)_3$, $\text{Gd}_2(\text{MoO}_4)_3$ and $\text{Eu}_2(\text{MoO}_4)_3$ crystals has been studied in situ using synchrotron radiation. All three isostructural compounds undergo a structural phase transition at 2.2–2.8 GPa to a new phase, which is interpreted as a possible precursor of amorphization. Amorphization in these crystals occurs irreversibly over a wide pressure range, and its mechanism, interpreted as a chemical decomposition, is found to be weakly affected by the degree of hydrostaticity.

© 2002 Elsevier Science Ltd. All rights reserved.

Keywords: A. Disordered systems; C. X-ray diffraction; D. Phase transitions; E. High pressure

1. Introduction

The investigation of pressure-induced solid-state amorphization is an important aspect of research in phase transitions at high pressure [1,2]. The number of substances found to become amorphous under high pressure is steadily increasing. The variety of compounds showing this effect, the conditions and features intrinsic to pressure-induced solid-state amorphization is surprising. In some substances amorphization is an irreversible process, with the sample remaining amorphous upon pressure release, while in others the crystal-to-amorphous transition is a perfectly reversible process. Furthermore, in many substances, reversibility, and even the occurrence of amorphization, depend considerably on the experimental conditions, especially on the hydro-

staticity of applied pressure. For example, amorphization in GeO_2 and in quartz does not occur under hydrostatic conditions in the pressure range where it was observed under non-hydrostatic stress [3,4].

Amorphization is not always easy to ascertain experimentally; the use of different experimental techniques to characterize amorphization, in particular to detect the existence of an amorphous phase, often provides contradictory evidence; e.g. one can find many examples of compounds in which low-frequency Raman spectroscopy data show absence of crystalline order while their X-ray diffraction patterns reveal well-defined Bragg peaks, indicating the presence of long-range periodic order [2]. Thus, only the use of a variety of analytical techniques will lead to conclusive insights into amorphization mechanisms, and to permit the separation of phenomena different in nature, but showing similar experimental signatures. In the past, amorphization mechanisms included vitrification, non-homogeneous macroscopic deformation, frustrated poly-morphic transition and chemical decomposition [1,2,6–8].

* Corresponding author. Address: Group “Structure of Materials under Extreme Conditions”, Swiss–Norwegian Beam Lines at ESRF, BP 220, F-38043 Grenoble, France. Fax: +33-476882694.

E-mail address: dmitriev@esrf.fr (V. Dmitriev).

In spite of the high level of research activity in the field, many features of pressure-induced amorphization are still unclear. This is the case, e.g. for, hydrostaticity which is considered to be a decisive factor in some mechanisms of break-up of long-range order. However, in a high-pressure experiment, even with special precautions, hydrostaticity cannot be ensured within the full pressure range of study. Thus, a clear understanding of how such a fundamental experimental factor affects different mechanisms of amorphization should be the first step (if not in time, but in logics) to develop an adequate model of amorphization in a compound, or in a crystal family. It would be of interest then to specify (a) the contributions from the initial grain structure, e.g. between single-crystal and polycrystalline states, (b) the contributions from non-hydrostatic stress components and temperature gradient, to the crystal-to-amorphous and amorphous-to-crystal transitions, and this in a series of substances related in crystal structure and physical properties.

To study these questions it seemed promising to investigate the rare-earth (RE) molybdates $R_2(\text{MoO}_4)_3$ family, where $R = \text{Pr, Nd, Sm, Eu, Gd, Tb, Dy}$. In the temperature range $1300 < T < 1500$ K, depending on the RE ion, these molybdates crystallize in the tetragonal β -phase (space group $P4_21m$, $Z = 4$) [8]. Below 1080–1260 K, the thermodynamically stable phase is the α -phase which has a monoclinic structure (S.G. $C2/c$, $Z = 12$). The transition to the equilibrium state upon cooling is frustrated due to low diffusive mobility of the metallic cations and a large volume effect at the transition (the density of the α -phase is larger by about 20% than that of the β -phase). The β -phase can thus be readily overcooled, even at low cooling rate. In the metastable β -phase, in the temperature range 418–508 K, a group-to-subgroup transition to an orthorhombic β' -phase (S.G. $Pba2$) takes place, with only a slight structural modification.

Amorphization for this class of compounds was first observed in $\text{Gd}_2(\text{MoO}_4)_3$ (GMO) by Brixner [9], who studied the structure of GMO thermally treated under pressure up to 6.0 GPa. He reported amorphization of the samples at $T < 670$ K. Later, Jayaraman et al. [5] and Ponyatovsky et al. [6,10] found that other members of this family, i.e. $\text{Tb}_2(\text{MoO}_4)_3$, $\text{Sm}_2(\text{MoO}_4)_3$, $\text{Eu}_2(\text{MoO}_4)_3$ and $\text{TbGd}(\text{MoO}_4)_3$, thermally treated at pressures up to about 7.0 GPa, also became amorphous. Amorphization of $\text{Tb}_2(\text{MoO}_4)_3$ was studied in situ by Jayaraman et al. using the Raman scattering and the energy-dispersive synchrotron radiation diffraction techniques [5]. The Raman study showed that in $\text{Tb}_2(\text{MoO}_4)_3$ amorphization is preceded by a polymorphic phase transformation at $P \approx 2.0$ GPa. However, the authors of Ref. [5] did not investigate in detail the structural evolution of $\text{Tb}_2(\text{MoO}_4)_3$ with pressure in the range of the crystal-to-crystal polymorphic transition and subsequent amorphization, because of a large fluorescence contribution of the Tb ions to the synchrotron radiation data.

Considering possible scenario of the amorphization

process, it should be noted that the decomposition of molybdate compounds to the corresponding metal oxides results in nearly the same volume decrease as the structural $\beta \rightarrow \alpha$ transition. Therefore, every mechanism, be it an impeded polymorphic transition or a sluggish decomposition, should be considered as the cause underlying the amorphization of the metastable β -phase with increasing pressure. Activation energy for the diffusion of the ions is an important factor determining the transformation paths for a compound.

The aim of the present work is to study in situ the process of pressure-induced amorphization in polycrystalline samples of $\text{Sm}_2(\text{MoO}_4)_3$, $\text{Gd}_2(\text{MoO}_4)_3$ and $\text{Eu}_2(\text{MoO}_4)_3$, in order to determine the role of hydrostaticity on amorphization.

2. Experimental

The structural study of the rare-earth molybdates was carried out on powdered samples obtained by grinding the corresponding single crystals grown from the melt by the Czochralsky techniques. Synchrotron radiation measurements were performed at the Swiss–Norwegian Beam Lines (BM1A) at the European Synchrotron Radiation Facility (ESRF, Grenoble, France) by angle-dispersive X-ray diffraction techniques using monochromatic X-ray radiation ($\lambda = 0.070053$ or 0.075 nm). The angular range measured spanned from 5 to $30^\circ 2\theta$. Pressure was generated using a gasketed diamond anvil cell with a gasket hole of $150 \mu\text{m}$ in diameter. The polycrystalline samples were placed into the gasket hole, together with ruby chips. Pressure was determined using the ruby fluorescence technique [11]. Measurements were carried out at room temperature in the pressure range up to 13.0 GPa. The $\text{Sm}_2(\text{MoO}_4)_3$ and $\text{Gd}_2(\text{MoO}_4)_3$ samples were studied without any pressure-transmitting medium, i.e. only under non-hydrostatic conditions.

Raman spectra of $\text{Eu}_2(\text{MoO}_4)_3$ single crystal were recorded in back-scattering geometry with a Dilor XY multichannel spectrometer equipped with a CCD detector. The 514.5 nm line from an Ar^+ ion laser was used as excitation source. High-pressure experiments were performed in a diamond-anvil cell with a 16:4:1 methanol–ethanol–water as pressure-transmitting medium. The sample was placed in a chamber $250 \mu\text{m}$ in diameter and $70 \mu\text{m}$ thick. Pressure was monitored with ruby chips placed in the vicinity of the sample.

The effect of hydrostaticity on the phase transformations was studied in detail using as an example $\text{Eu}_2(\text{MoO}_4)_3$: non-hydrostatic experiments on $\text{Eu}_2(\text{MoO}_4)_3$ was followed by measurements using silicon oil or 4:1 ethanol–methanol mixture as pressure transmitting media. Silicon oil is known to stiffen into a rigid solid around 2.5 GPa at room temperature. Thus, the $\text{Eu}_2(\text{MoO}_4)_3$ compound was studied under non-hydrostatic conditions (without any transmitting medium),

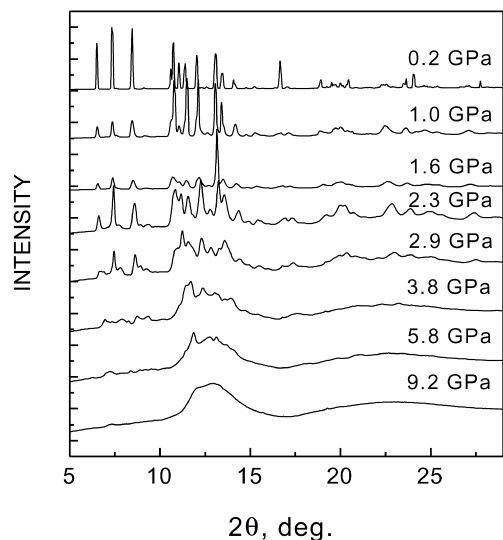


Fig. 1. Evolution of X-ray powder diffraction patterns for $\text{Sm}_2(\text{MoO}_4)_3$. The data at each pressure are normalized on the peak with maximum intensity.

under low hydrostaticity (with the silicon oil medium) and under hydrostatic conditions (in the alcohol mixture).

3. Results

Figs. 1–3 show diffraction patterns of $\text{Sm}_2(\text{MoO}_4)_3$, $\text{Gd}_2(\text{MoO}_4)_3$ and $\text{Eu}_2(\text{MoO}_4)_3$ powders obtained under non-hydrostatic conditions. One can conclude, from the figures, that the amorphization process is very similar in all the three RE molybdate compounds. The behavior of the experimental diffraction spectra indicates the identity of the structural changes upon amorphization. Three intervals can be identified over the pressure range studied, which characterize different states of the compounds.

3.1. Orthorhombic-to-monoclinic phase transition

In the *first* interval (pressure ambient to 2.5 GPa), the diffraction patterns correspond to the orthorhombic β' -phase, and the pressure increase results only in a lattice contraction. Additional reflections in the diffraction patterns arise in the pressure range 2.2–2.8 GPa, indicating a transition to a new phase, δ (we do not use the designation γ for this phase, to avoid confusion with the γ phase in $\text{Dy}_2(\text{MoO}_4)_3$ at atmospheric pressure). Fig. 4 shows in detail the evolution of the low-angular range $2\theta = 6.0\text{--}10.0^\circ$ of the $\text{Eu}_2(\text{MoO}_4)_3$ under hydrostatic conditions and $\text{Sm}_2(\text{MoO}_4)_3$ under non-hydrostatic ones. The $\beta' \rightarrow \delta$ phase transition in these compounds definitely occurs around $P = 2.5$ GPa; this is evident, for example, from the splitting of the (111) reflection or the (021) group of reflections. These splittings indicate that the symmetry of

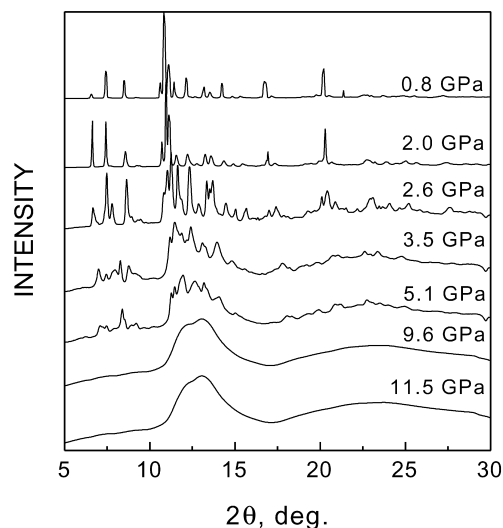


Fig. 2. Evolution of X-ray powder diffraction patterns for $\text{Gd}_2(\text{MoO}_4)_3$. The data at each pressure are normalized on the peak with maximum intensity.

the lattice in the δ phase is lowered to monoclinic or, possibly, triclinic. Additional lines also develop as a shoulder on the high-angle side of the (002) peak. However, the quality of the powder diffraction data is not sufficient to solve the structure of this new phase. The single crystal experiments are actually in progress and the corresponding results will be published soon.

In order to establish the analogy between the structure transformations at about 2.5 GPa for different RE molybdates, we carried out a Raman scattering study on a single crystal $\text{Eu}_2(\text{MoO}_4)_3$. Fig. 5 presents the evolution of the

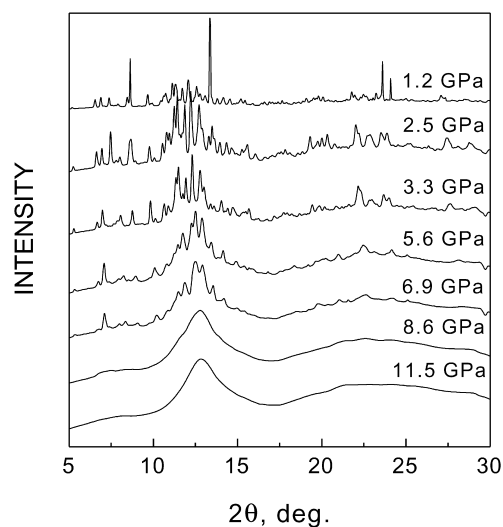


Fig. 3. Evolution of X-ray powder diffraction patterns for $\text{Eu}_2(\text{MoO}_4)_3$. The data at each pressure are normalized on the peak with maximum intensity.

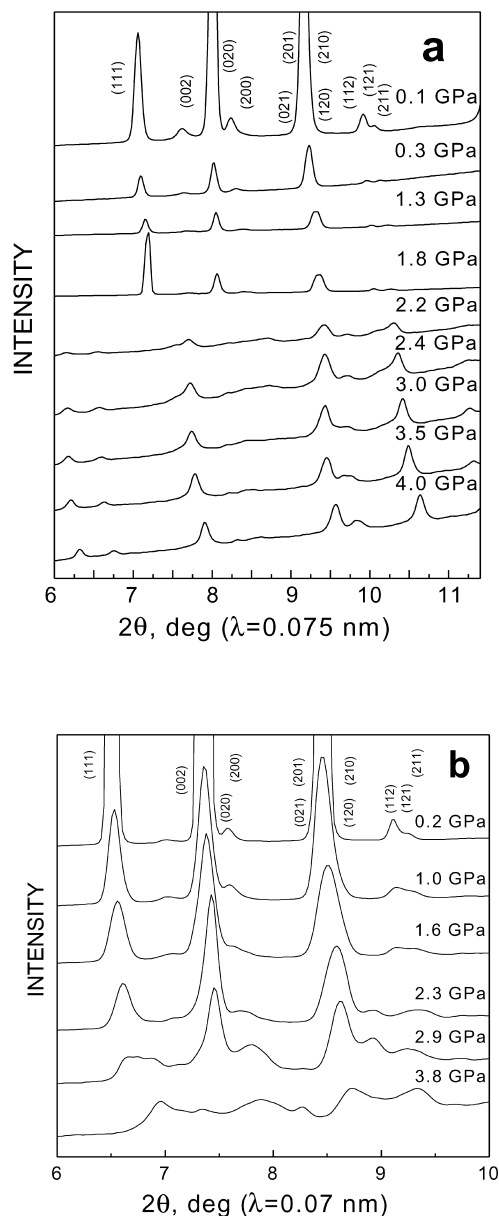


Fig. 4. Evolution of the X-ray diffraction patterns for $\text{Eu}_2(\text{MoO}_4)_3$ (a) and $\text{Sm}_2(\text{MoO}_4)_3$ (b) in the pressure range of the orthorhombic-to-monoclinic phase transformation. The wavelength of the X-ray radiation was (a) 0.075 nm; (b) 0.070053 nm.

single crystal Raman spectra with the applied hydrostatic pressure up to 6.8 GPa. At ambient pressure, the Raman spectra fit well with the orthorhombic phase of the isostructural compound $\text{Gd}_2(\text{MoO}_4)_3$ [12]. At $P = 2.0$ GPa, significant changes occur in the spectra: appearance of new lines in the $850\text{--}900\text{ cm}^{-1}$ region and disappearance of lines in $830\text{--}850\text{ cm}^{-1}$ region. With increasing pressure up to 6.2 GPa, Raman spectra become similar to those of the new monoclinic phase reported for $\text{Tb}_2(\text{MoO}_4)_3$ [5], thus it

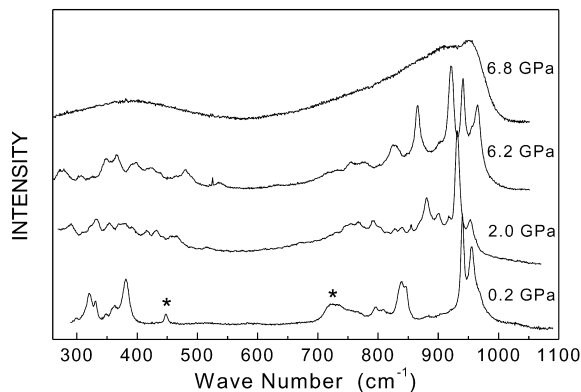


Fig. 5. Pressure evolution of the Raman spectra of the single crystalline $\text{Eu}_2(\text{MoO}_4)_3$. Asterisks denote Eu^{3+} fluorescence bands.

is natural to suggest that the δ -phase is isostructural for all RE molybdates.

3.2. Pre-amorphization effects

In the *second* pressure interval, between 2.8 and 8.0 GPa, just above the $\beta' \rightarrow \delta$ phase transition, the X-ray diffraction peaks gradually broaden, and the background rises with increasing pressure. The Bragg peaks degenerate fully, and characteristic diffuse halo appears around 8.0 GPa for all the compounds studied, indicating that the transformation to the amorphous state is complete. However, an exact localization of P - T conditions for the transition to the amorphous state is difficult to determine, because of the sluggishness of the transition. In contrast with the classic X-ray diffraction pattern for a glassy material, the first diffuse diffraction halo in the amorphous state has a complex shape, which is indicative of a structural inhomogeneity in the first coordination shell. It should be noted that in the Raman spectra drastic change occurs within a short range of pressure, when the crystal-to-amorphous transformation begins. All Raman peaks corresponding to the internal vibrations of the Mo-O tetrahedra broaden (in the $800\text{--}1000\text{ cm}^{-1}$ region), while the peaks in the external mode region $200\text{--}400\text{ cm}^{-1}$ disappear (Fig. 5).

3.3. Amorphous state

The amorphous state of the RE molybdates persists over the *third* pressure interval (8.0–13.0 GPa), with the first diffraction halo changing somewhat in its shape. To test the possibility of recrystallization of the amorphous phase we annealed the samples under the pressure $P = 13.0$ GPa at $T = 450$ K for 2 h. This procedure, however, did not result in the re-appearance of Bragg peaks but, on the contrary, led to a complete degeneration of the structure of the diffuse halo, indicating progressive disorder in the structure.

When silicon oil was used as the pressure-transmitting medium, the evolution of the diffraction spectrum under

pressure was very similar to that observed under the quasi-hydrostatic conditions. The values of the transition pressures to the new high-pressure phase δ and to the amorphous state were much the same. Under hydrostatic conditions with the alcohol mixture, amorphization was observed again, but the baric evolution of the diffraction peak parameters was rather different from those under the quasi-hydrostatic conditions. In this case, the Bragg peaks broadened only weakly up to the transition to the amorphous state, and increasing pressure resulted only in an increase of the background.

Upon release of pressure down to ambient, all three molybdates remained in the amorphous state as indicated by the broadened high-frequency Raman bands, and the transformation is irreversible.

4. Discussion

In the RE molybdate compounds, the initial crystalline order may break down along three different mechanisms, namely, (a) mechanical deformation, (b) chemical decomposition and (c) crystallographic transformation. The *mechanical* process implies a non-homogeneous macroscopic deformation of a crystalline sample by non-hydrostatic shear components, whereas the short-range chemical order, which existed in the original crystal unit cell, is preserved. The second mechanism is *decomposition* of an initially complex compound into simpler components and, in our case, this would be the decomposition of $R_2(\text{MoO}_4)_3$ molybdate into $R_2\text{O}_3$ and MoO_3 oxides. The feature common to the two processes just mentioned is that it is not a new thermodynamic state of the *original* crystal. Finally, the *crystallographic* mechanism leads to a disorder in the crystal structure, both orientational and positional, but without any *substantial* atomic displacements or diffusion, and without change in the initial chemical composition. The final disordered isotropic state should be considered as a new phase (stable or metastable). The onset of an intermediate, non-crystalline state between two crystal phases (due to a kinetically impeded structural phase transition) can also be considered, formally and under special conditions, as a crystallographic process.

When it comes to deciding which mechanisms is the operative one in our case, two features of the above mechanisms are of particular relevance, as we will see later: the effect of hydrostaticity on the crystal-to-amorphous transformation and the reversibility of the transformation.

(a) *Mechanical deformation*. In the case of our RE molybdates, hydrostaticity (or lack thereof) seems to have little effect, as amorphization occurs independently of the nature of the applied stress, and remains upon release of pressure. The mechanical scenario of amorphization is thus not sustainable and can be excluded, despite the fact that application of inhomogeneous stress results in a strong broadening of the X-ray reflections; this broadening,

however, is solely indicative of slight lattice distortions. The polymorphic phase transition at $P \approx 2.2\text{--}2.8$ GPa is interpreted here as a phenomenon precursory to amorphization. The resulting low-symmetry phase amorphizes upon further pressure increase. Finally, the irreversible character of the transformation is also not consistent with a mechanical scenario.

(b) *Chemical decomposition*. Irreversibility of the transformation, on the other hand, is consistent with chemical decomposition; as high-energy barriers prevent the reverse process, synthesis from the oxides, from taking place. However, the mere observation of irreversibility is not sufficient to decide unambiguously in favor of chemical decomposition. The *first step* in chemical decomposition is incipient segregation, which is similar to crystallographic disordering. Both processes differ mainly in the heights of the energy barriers to be overcome by atoms. At this early stage, the transformation product, if annealed at ambient pressure in the stability region of the initial crystalline structure, recrystallizes in this structure, as was observed, for example, by Brixner for GMO [9]. The barriers at this stage can be either low enough to allow reversibility of the transformation, or attain a magnitude such as to impede the reverse amorphous-to-crystal transformation. Thus, irreversibility is a necessary but not sufficient criterion.

(c) *Crystallographic transformation*. In the crystallographic mechanism, non-hydrostatic stress components, due to their symmetry properties, can be conjugated (coupled) to the elastic order parameter [13]. Such a selective resonance type coupling between the non-hydrostatic stress components and order parameter components can induce, in turn, the onset of a lattice shear instability, triggering the amorphization of the crystal [13], and this is even for a relatively small amount of non-hydrostaticity.

In contrast, the chemical decomposition mechanism, which cannot be characterized by a symmetry, the cumulative *magnitude* of pressure, destabilizing a compound, plays a much more important role than the ratio between its symmetrically different hydrostatic and non-hydrostatic addends. Thus, the vanishingly small effect of non-hydrostaticity, even if cannot be ruled out unequivocally, speaks in favor of the mechanism of chemical decomposition. Most of the evidence obtained so far point to chemical decomposition as the operative mechanism. To firm up this claim, we subjected europium molybdate to additional experiments. The material was first pressed up to the onset of the amorphous state (10.0 GPa). Then the amorphized samples were annealed in an atmosphere of various gases, such as O_2 , Ar or He, and under different temperatures. In all cases, we observed a progressive recrystallization at temperatures higher than 750 K. Fig. 6 shows an X-ray powder diffraction pattern of initially amorphous europium molybdate, but subsequently annealed at 900 K during 2 h. One observes that the most intensive peaks belong to the orthorhombic (slightly distorted cubic) form of europium oxide, Eu_2O_3 , while the less intense ones

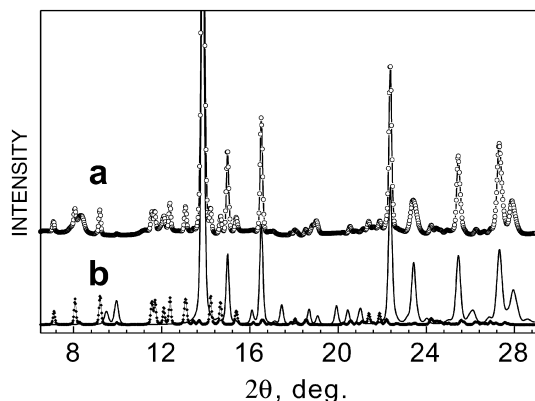


Fig. 6. X-ray diffraction patterns of $\text{Eu}_2(\text{MoO}_4)_3$, amorphized and then annealed at ambient pressure: (a) experimental diffractogram; (b) simulated patterns of Eu_2O_3 (solid line) and β' - $\text{Eu}_2(\text{MoO}_4)_3$ (diamonds).

fit well with the β' -structure of $\text{Eu}_2(\text{MoO}_4)_3$. Although the diffraction data are not yet of a quality such that a full Rietveld, multiphase refinement can be carried out, the distinct presence of Eu_2O_3 strongly supports the chemical decomposition mechanism. MoO_3 is most certainly also present, but unfortunately many of its diffraction lines coincide with the Eu_2O_3 ones. Keeping in mind the results published by Brixner [9], we suggest that the region of chemical instability of the RE molybdates is limited to high temperatures, in the temperature region where the crystalline α -phase is stable. In this case high-temperature–high-pressure annealing (Brixner's procedure) drives the system into the α -phase, while room-temperature–high-pressure treating promotes the chemical decomposition disclosed in our experiment.

In conclusion, we suggest the following scenario for the amorphization process in the crystals of this family, a mechanism which is maximally compatible with our experimental data. The new δ -phase formed under pressure is both thermodynamically and chemically unstable with respect to decomposition of $\text{R}_2(\text{MoO}_4)_3$ to R_2O_3 and MoO_3 . The amorphization process starts in the most defect-rich regions of the samples like grain surfaces, domain boundaries, etc. Concomitant with the nucleation and the growth of the amorphous layer is a rise of an internal stress at the crystal/amorphous boundary, which results in the formation of a wide two-phase pressure range. Due to the presence of this two-phase δ /amorphous state in the samples, the atomic structure of the δ -phase could not yet

be determined, in spite of its importance for an understanding the mechanism of amorphization. It is of a great interest therefore to study in situ the process of amorphization of these compounds under high pressure, over a wide range of temperatures. If the amorphous state is formed due to decomposition we will again observe the appearance of R_2O_3 and MoO_3 oxides. If the crystallographic mechanism is the operative one, we will obtain a denser crystalline modification with a change in the coordination number of the molybdenum ions. Such experiments are planned in the near future.

Acknowledgments

This work was supported in part by the Swiss Scientific Program SCOPES-2000 (Project No. 7SUPJ062362) and by RFBR (Grant No. 99-02-17007). Experimental assistance from the staff of the Swiss–Norwegian Beam Lines at ESRF is gratefully acknowledged.

References

- [1] E.G. Ponyatovsky, O.I. Barkalov, Mater. Sci. Rep. 8 (1992) 147–191.
- [2] S.M. Sharma, S.K. Sikka, Progr. Mater. Sci. 40 (1996) 1–77.
- [3] V.V. Brazhkin, E.V. Tat'yandin, A.G. Lyapin, S.V. Popova, O.B. Tsoik, D.V. Balitskii, JETP Lett. 71 (2000) 293–297.
- [4] J. Haines, J.M. Leger, F. Gorelli, M. Hanfland, Phys. Rev. Lett. 87 (2001) 155503/1–155503/4.
- [5] A. Jayaraman, S.K. Sharma, Z. Wang, S.Y. Wang, L.C. Ming, M.H. Manghnani, J. Phys. Chem. Solids 54 (1993) 827–833.
- [6] E.G. Ponyatovsky, V.V. Sinitsyn, R.A. Dilanyan, B.S. Red'kin, JETP Lett. 61 (1995) 222–226.
- [7] A.K. Arora, Solid State Commun. 115 (2000) 665–668.
- [8] L.H. Brixner, J.R. Barkley, W. Jeitschko, in: K.A. Gscheidner Jr., L.R. Eyring (Eds.), Handbook on the Physics and Chemistry of Rare Earths, vol. 610, 1979, Chapter 30.
- [9] L.H. Brixner, Mater. Res. Bull. 7 (1972) 879–885.
- [10] A.V. Pal'nichenko, E.G. Ponyatovsky, B.S. Red'kin, V.V. Sinitsyn, JETP Lett. 68 (1998) 657–661.
- [11] G.J. Piermarini, S. Block, J.D. Barnett, R.A. Forman, J. Appl. Phys. 46 (1975) 2774–2780.
- [12] B.N. Ganguly, F.G. Ullman, R.D. Kirby, J.R. Hardy, Phys. Rev. B 13 (1976) 1344–1352.
- [13] N. Binggeli, J.R. Chelikowsky, Phys. Rev. Lett. 69 (1992) 2220–2223.